Evaluating Ammonia as Green Fuel for Power Generation: A Thermo-chemical Perspective

Antonio Sánchez[a], Elena Castellano[a], Mariano Martín[a,*], Pastora Vega[b]

[a]*Department of Chemical Engineering, University of Salamanca, 37008 Salamanca, Spain*
[b]*Department of Computer Science, University of Salamanca, 37008 Salamanca, Spain*

Abstract

Energy storage will be necessary for a future power system with high penetration of renewable sources, mainly, wind and solar, to ensure the stability of the grid. In this context, power-to-chemicals is a promising concept for a medium/long-term storage horizon and a wide range of capacities. Within this alternative, ammonia rises as one of the fuels with the highest potential in a scenario targeting decarbonization. The first step is the production of ammonia using renewable energy sources, followed by its transformation into energy. This second area requires a deeper analysis at process scale in order to introduce this technology into the future power system. In this work, an assessment of an ammonia-based power plant is presented, focusing on the thermo-chemical route. A combined cycle is evaluated, considering different gas clean-up technologies to recover valuable components and comply with environmental restrictions. As a result, the total efficiency of the power facility reaches about 40%, limited by the maximum temperature allowed in the gas turbine. The influence of the price of ammonia is also evaluated due to the paramount importance of this parameter. The production cost ranges from 0.2 to 0.6 €/kWh, with the lowest level corresponding to a scenario in which there is a significant reduction in the cost of renewable power generation and electrolysis technology. Therefore, the feasibility of the use of ammonia as an energy storage alternative is demonstrated, providing a powerful platform for the implementation of a power grid with high penetration of fluctuating sources.

Keywords: Ammonia Combustion, Energy Storage, Green Ammonia, Power-to-X, Power Generation, Renewable Fuels

*Corresponding author
Email address: mariano.m3@usal.es (Mariano Martín)

1. Introduction

An increase in the share of renewable energy sources (RES) is expected in the coming years to meet the global sustainable goals (UN General Assembly, 2015). Current predictions indicate that, in 2050, 69% of the power will be produced from RES, being wind and solar the two main sources with 56% of the total share (BloombergNEF, 2020). The penetration is not homogeneous across the different territories. The deepest and fastest energy transition will take place in Europe, where 74% of the power will be generated using PV panels and wind turbines by 2050. The main challenges of an energy system with high penetration of these RES are the random variability of the solar/wind resources and the imbalance between power generation and electricity consumption. Therefore, a combination of intermittent and non-intermittent RES and different storage technologies is required to ensure the robustness of the grid (Child et al., 2019). Hence, different energy storage technologies have been proposed to mitigate the fluctuations in power production (Frate et al., 2021; Gür, 2018). For a day/week/month/seasonal storage, power-to-chemicals alternatives are receiving attention due to the high energy density of these fuels, the possibility of easy storage and transportation of these products, and the scalable and flexible behavior of this storage alternative.

Hydrogen has been proposed as one of the key elements in the next energy system for grid-scale storage (Zhang et al., 2019; Pellow et al., 2015), and also for transportation (Ehrenstein et al., 2020). A major boost to the hydrogen economy is expected in the coming years, mainly in Europe, where the post-COVID European Green Deal introduces the goal of making the old continent the first climate-neutral territory by 2050 (van Renssen, 2020). The European hydrogen strategy foresees a cumulative investment in renewable hydrogen up to €470 billion by 2050 (European Commission, 2020). At this point, the development of a competitive electrolysis technology is crucial for the implementation of this path (Mohammadi and Mehrpooya, 2018). To convert H_2 into power, fuel cells are the most extended technology (Zhang et al., 2020). However, one of the main challenges is the temporary storage of hydrogen. Several options have been proposed, for example, high-pressure gas tanks (Götz et al., 2016) or metal hydrides (Heras and Martín, 2021). In addition, different hydrogen-based derived products have been proposed which are easier to store and transport. Methane received attention due to the existing infrastructure to distribute natural gas. This hydrogen carrier can be produced through methanation using H_2 and CO_2 (Sternberg and Bardow, 2016; Davis and Martín, 2014). Other carbon-based carriers as methanol (Al-Qahtani et al., 2020; Daggash et al., 2018) or DME (Dieterich et al., 2020; Martín, 2016) have also been evaluated. Moreover, different technologies have been proposed to convert these fuels into power, for instance, gas turbines or fuel cells (Wang et al., 2020).

In particular, one of the hydrogen carriers that is attracting more attention is ammonia since it is a high energy density fuel, with simple storage and with no CO_2 associated emissions (Palys et al., 2021; Cesaro et al., 2021; Fúnez Guerra et al., 2020). Some safety issues have been reported on the use of ammonia as fuel (Di Sarli et al., 2017), however, industrial experience with this chemical turns ammonia into a safe fuel with risks and hazards similar to others such as gasoline or LPG (MacFarlane et al., 2020). Several works have analyzed the synthesis of ammonia using renewable power (Sánchez and Martín, 2018a; Allman and Daoutidis, 2018; Wang et al., 2017). After its production, the next stage is to transform it into power when renewable generation is low (Valera-Medina et al., 2018). Two main options are proposed: technologies based on ammonia fuel cells (electro-chemical) and combustion (thermo-chemical). Siddiqui and Dincer (2020) conducted an experimental evaluation of an integrated system, in which, ammonia is synthesized on-site and used directly in a fuel cell. Furthermore, different hydrogen/ammonia blends have also been evaluated to improve the performance of the system (Siddiqui et al., 2020). In this area, Jeerh et al. (2021) review the different fuel cell technologies in which ammonia can be used as fuel. Solid oxide fuel cells (SOFC) rise, to date, as the most promising alternative in ammonia fuel cells. Regarding combustion, Kobayashi et al. (2019) summarized the main experimental advances in ammonia combustion in recent years. Different ammonia/methane (Valera-Medina et al., 2017) and ammonia/hydrogen (Valera-Medina et al., 2019) blends have been proposed as fuel mixtures for gas turbines to overcome the challenges in ammonia combustion. A thermodynamic analysis of an ammonia-fueled gas turbine is presented by Keller et al. (2020). Furthermore, ammonia-based internal combustion engines have also been proposed to be used in transportation applications (Mounaïm-Rousselle and Brequigny, 2020). Lastly, some authors proposed an integration of both methods to produce power from ammonia (Ezzat and Dincer, 2020). However, most of these analyses are experimental and only evaluate the major unit of the ammonia-to-power process. Therefore, an analysis at process scale is required to assess the entire transformation of ammonia into power including the preparation of the raw materials, the transformation into power, and the subsequent treatments, in order to ensure the economic and environmental feasibility of the process. With these studies, it is possible to evaluate the performance of the entire facility, determining the total energy efficiency of the process and the cost of the electricity for the different technologies. These assessments are mandatory to be able to introduce these technologies in real applications and, to the best of our knowledge, no specific research in this area is available in the literature.

In this work, a process level analysis of the production of power from ammonia using the thermo-chemical path is presented. Particularly, a combined cycle is analyzed

using a fuel blend consisting on ammonia and hydrogen. The decomposition of the ammonia to produce the necessary hydrogen is also evaluated in this work. Additionally, different gas cleanup technologies have also been examined. The process superstructure is optimized to determine the optimal path and operating conditions of the ammonia-to-power transformation. After the optimization, some additional sensitivity and scale up studies are carried out to evaluate the technical performance of the process and the economics of this new power generation alternative.

2. Process Description

The process of converting ammonia into power is divided into four main sections: fuel mixture preparation, combined cycle (gas and steam turbines), gas clean-up, and N_2/Ar separation (as shown in Figure 1). In the first section, the fuel mixture is prepared according to the features required by the combustion of ammonia. As it has been previously mentioned, ammonia is a relatively unreacted fuel and, therefore, a mixture of hydrogen and ammonia is used in this work as a feed for the combined cycle. This mixture is selected versus other alternatives, such as the ammonia/methane blends, in order to maintain the carbon-free power generation using ammonia. Particularly, a blend of 70% of ammonia and 30% of hydrogen is selected in this work to overcome the ignition and burning velocity issues of the combustion of ammonia alone (Valera-Medina et al., 2019). To produce the necessary hydrogen, ammonia decomposition is employed to be able to operate the facility with ammonia alone as feedstock. To decompose ammonia, a catalytic membrane reactor is set up. Inside the reactor, ammonia is broken down into nitrogen and hydrogen, the two initial constituents, and hydrogen is recovered in the same unit using an appropriate membrane (Jo et al., 2018; Chiuta et al., 2013). Two outlet streams are obtained from the reactor: the first one, which contains hydrogen that is used in the NH_3/H_2 fuel mixture, and the second one, which is composed mainly of nitrogen and also some small amounts of hydrogen and ammonia. This last stream can be recycled to the ammonia production and be used in the synthesis loop, reducing the production cost of renewable ammonia.

The blend, that is introduced into the gas turbine, is made up of hydrogen and ammonia, air and argon. Argon is fed to control the maximum temperature inside the gas turbine. If the mixture of ammonia/hydrogen is burnt as such, an outlet temperature of about 2100ºC is reached (Otomo et al., 2018). However, this value is too high for the traditional gas turbine systems, mainly due to material limitations. Therefore, the maximum temperature in the combustion chamber is limited to 1600ºC in this work (Gu et al., 2016). Other inerts, instead of argon, have also been evaluated as carbon dioxide or nitrogen. The first is discarded in order to generate power without any carbon

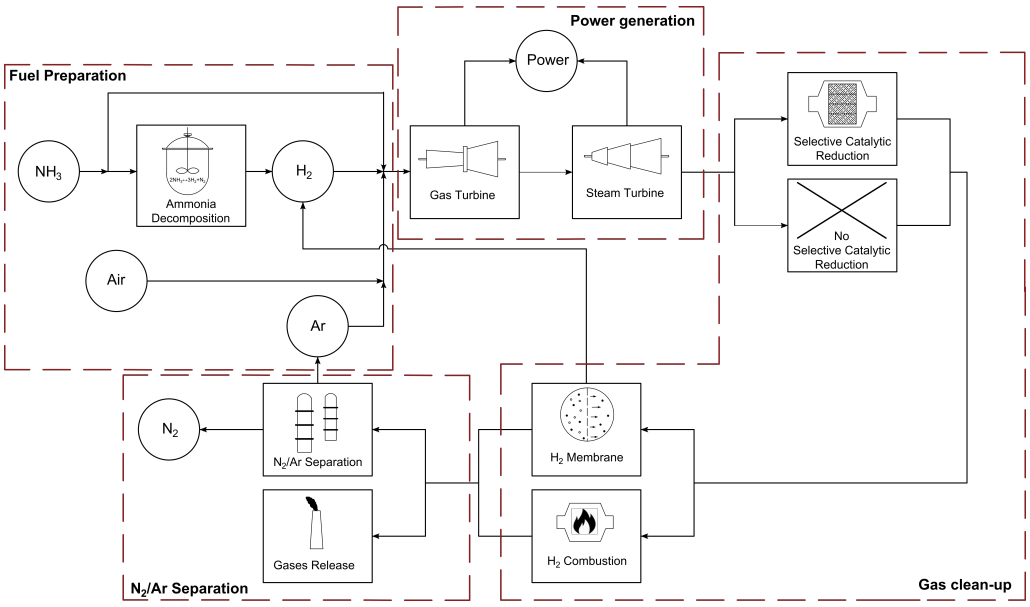

Figure 1: Process superstructure diagram for ammonia-to-power transformation

component involved. The second, due to the problem of the formation of nitrogen oxides in the ammonia combustion (as explained below), that could be amplified if larger amounts of nitrogen are introduced into the combustion chamber.

The inlet gas mixture is introduced into the first step of the combined cycle: the gas turbine. Within this unit, the inlet gases are compressed, the combustion of the hydrogen/ammonia mixture takes place and the gases from the combustion chamber are expanded to produce power (Ezzat and Dincer, 2020). The outlet gases from the gas turbine are fed into the Rankine cycle. Three different sections of the steam turbine are considered in this work with various operating pressures (high, medium and low pressure).

After the Rankine cycle, some operations to clean-up the gases are required. The first one is related to the NO_x produced during the ammonia combustion. In the superstructure proposed, it is possible to remove the nitrogen oxides by selective catalytic reduction (SCR) (Resitoglu and Keskin, 2017). If the emission limit values for this pollutant (European Council, 2010) are met without the treatment, it is possible to discard this unit, and a bypass is considered. The next step in the gas clean-up section is hydrogen recovery. This stage is required because one of the products leaving ammonia combustion is hydrogen, which is a valuable component that should be recovered during gas treatment. In this study, two different options are evaluated. On the one hand, hydrogen could be separated using a membrane and recycled to the fuel mixture preparation

section. On the other hand, hydrogen is burnt and the energy released during this step is used to reheat the steam within the Rankine cycle allowing for larger power generation.

Finally, the gases can be released into the atmosphere in compliance with environmental restrictions. In this case, nitrogen and argon cannot be reused in the ammonia synthesis and combustion, respectively. Another alternative is to separate the final gas stream, mainly nitrogen and argon, to be able to reuse nitrogen in the ammonia synthesis and to recycle argon for ammonia combustion. To perform this separation, cryogenic distillation is selected in this work.

3. Modelling Issues

This section presents a brief description of the different approaches to modeling the units involved in the NH_3-to-power superstructure. The modeling is based on mass and energy balances and the most relevant details are presented in this section.

3.1. Ammonia Decomposition Reactor

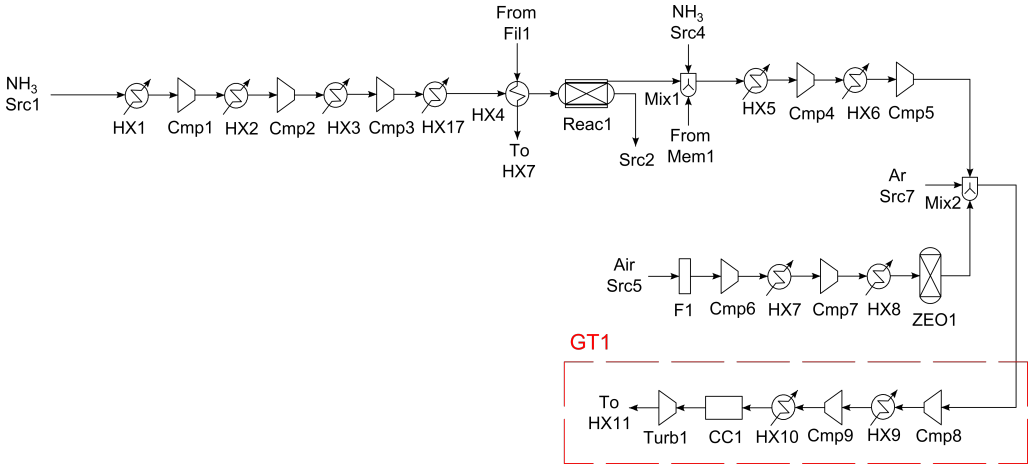

Figure 2: Process flow diagram for ammonia decomposition and gas turbine sections

In the decomposition reactor (as shown in Figure 2), ammonia is converted into nitrogen and hydrogen according to the following reaction:

$$NH_3 \leftrightarrow \frac{1}{2}N_2 + \frac{3}{2}H_2 \tag{1}$$

This stage is carried out in a fixed-bed isothermal membrane reactor (Li et al., 2013). The catalyst used is Ni/Al_2O_3, which gives a good performance in ammonia decompo-

sition, is a cheap metal, and is widely accepted as an economical alternative to ruthenium catalysts (Chiuta et al., 2013). A H_2-selective membrane is installed to separate the H_2 in the same unit. A Pd-Ag supported membrane is selected in this study (De Falco et al., 2011). The kinetic equation for the ammonia decomposition is adapted from the Temkin expression (Kim et al., 2018).

$$r = 3k_{reac}\left[K_p^2 a_{N_2}\left(\frac{a_{H_2}^3}{a_{NH_3}^2}\right)^{\alpha} - \left(\frac{a_{NH_3}^2}{a_{H_2}^3}\right)^{1-\alpha}\right]\Phi\Omega \tag{2}$$

The permeation rate of H_2 through the membrane is expressed as a function of the gradient of partial pressure on both sides (Abashar, 2018).

$$r_{H_2}^p = \left(\frac{28.84\times10^{-5}}{\delta}\right)exp\left(\frac{-1888.381}{T}\right)\left(\sqrt{P_{H_2}^r} - \sqrt{P_{H_2}^p}\right) \tag{3}$$

The pressure on the permeate side is fixed to 1 bar. With the kinetic expressions, the model of the membrane reactor consists of five differential equations, three for the mass balances of each of the components, the energy balance and the momentum balance computed with the Ergun equation for the catalytic side. The details of the model are presented in the Supporting Information. However, this model is too complex to be introduced in the optimization of the entire superstructure. To solve this issue and following the approach proposed by Paixão et al. (2018), metamodels or surrogate models were generated using the more rigorous model with the differential equations. Specifically, polynomial regression models have been selected for this case. The general formula to describe this kind of surrogate models is as follows (Sánchez et al., 2020):

$$f(x) = \beta_0 + \sum_{i=1}^{n}\beta_i x_i + \sum_{i=1}^{n}\sum_{j\leq i}^{n}\beta_{ij}x_i x_j \tag{4}$$

Four different variables have been considered as inputs for these models: inlet pressure (P) and temperature (T), inlet gas velocity (v_{reac}) and the total conversion (X_{total}), that represents the percentage of recovered hydrogen through the membrane versus the total hydrogen contained in the inlet ammonia. The objective is to calculate the conversion in the fixed bed (X_{reac}) and the length of the reactor (L_{reac}). The p-value determines the significant coefficients in the model for each case. The surrogate models generated for each output variable are:

$$\begin{aligned} X_{reac} = {} & -2.305 - 0.0060P + 0.0051T + 0.0010v_{reac} + 2.744X_{total} \\ & - 1.424\times10^{-6}T^2 + 3.884\times10^{-6}PT + 0.0040PX_{total} - 0.0033TX_{total} \end{aligned} \tag{5}$$

$$L_{reac} = 442.6363 + 1.1719P - 1.1936T + 12.7908v_{reac} + 31.7269X_{total} + 0.00076T^2 - 0.00077PT - 0.05051Pv_{reac} - 0.62543PX_{total} - 0.02251Tv_{reac} + 13.8569v_{reac}X_{total} \quad (6)$$

These two surrogate models have been developed for the following ranges of the input variables: inlet temperature between 700-850 K, inlet pressure 10-50 bar, inlet gas velocity in the range of 0.85-1.5 m/s and the total conversion between 0.85-0.95.

3.2. Gas turbine

The gas turbine (as shown in Figure 2) is modeled using three different sections. Firstly, a multistage compression stage with intercooling, the second step is the combustion chamber and the last one, the expansion to produce power (León and Martín, 2016). Polytropic compression and expansion are assumed for the gases with a polytropic coefficient (k) equal to 1.4 and the efficiency of the process is fixed to 0.85. One of the key points in this section is to model the ammonia/hydrogen combustion. In this work, the mixture is burnt with air in the presence of argon, as an inert, to reduce the outlet temperature. The amount of air that is necessary to introduce is based on the selected equivalent ratio (ER). This parameter represents the ratio between the stoichiometric oxygen and the real one introduced into the combustion chamber. In this work, and according to previous experimental results (Khateeb et al., 2020; Valera-Medina et al., 2019), the ER is limited within the range of 1.2-1.4. As products of the combustion, nitrogen and water are the most representative. It is assumed that ammonia is not in the outlet gases (Otomo et al., 2018). The amount of each component and the final temperature is computed using mass and energy balances. As mentioned above, the maximum temperature at the combustion chamber is limited to 1600ºC. One of the main limitations in ammonia combustion is the formation of nitrogen oxides. To compute the amount of this pollutant generated in the combustion chamber, an empirical correlation is developed, based on experimental results from Valera-Medina et al. (2019), where the nitrogen oxide concentration in the outlet gases is a function of the ER (for the range used in this work).

$$NO(ppm) = 2.9951 \times 10^{19} exp(-31.9846ER) \quad (7)$$

3.3. Rankine cycle

After the gas turbine, the gases are introduced into the Rankine cycle in order to increase the efficiency of power production (as shown in Figure 3). High, medium and low pressure steam turbines (Meroueh and Chen, 2020) are introduced to represent the multistage expansion in a real steam turbine. The high-pressure unit operates between

95-125 bar in the inlet stream, the medium pressure in the range of 11-35 bar and the low pressure between 5-9.5 bar, common ranges in the operation of the Rankine cycle. The gases from the gas turbine are used to heat up and evaporate the steam. To compute the enthalpies and entropies of each of the streams involved in the Rankine cycle, the proposed correlations by León and Martín (2016) were used where the enthalpy/entropy is a function of pressure and temperature. In each of the turbines, the isoentropic efficiency is fixed to 0.9 (Sadi and Arabkoohsar, 2019).

3.4. Gas cleanup

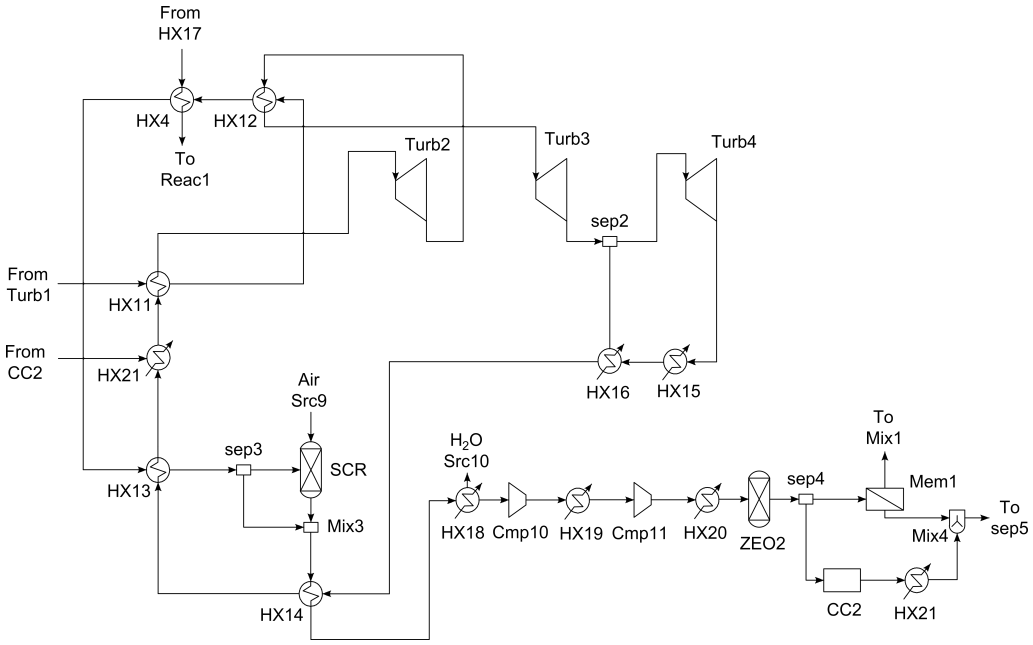

Figure 3: Process flow diagram for Rankine cycle and gas cleanup section

Nitrogen oxides are produced during ammonia combustion. This is a significant pollutant and must meet strict regulation. In the proposed superstructure (as shown in Figure 3), there are two possible options: the first one is to use a nitrogen oxide abatement technology to remove it and the second one is not to use any as long as the flue gas complies with environmental restrictions. To remove the nitrogen oxides, different treatments have been proposed (Guerras and Martín, 2019). In this study, a selective catalytic reduction (SCR) using hydrogen is selected. Hydrogen is chosen over ammonia or other products because it is a product of ammonia combustion and is presented in the gas stream. In addition, only small amounts of hydrogen are required for this treatment because of the reduced concentration of NO_x. The subsequent reaction takes

places in the SCR reactor (Resitoglu and Keskin, 2017):

$$2NO + 4H_2 + O_2 \rightarrow N_2 + 4H_2O \tag{8}$$

A conversion of 100% is assumed in this work. The second stage in the gas cleanup section is related to the recovery of hydrogen. Significant amounts of this chemical leave the combustion chamber of the gas turbine, however, hydrogen is a valuable component and should be recovered. Two options have been proposed for this stage. Firstly, hydrogen can be separated using a membrane and recycled to the fuel mixture preparation section. A separation factor for H_2 equal to 68 is fixed, with an operating pressure of 6 bar (Zhu et al., 2017). The second option is to burn the hydrogen to reheat the steam within the Rankine cycle (in the heat exchanger HX21 before the high pressure steam turbine). If more heat is introduced into the cycle, higher power production is expected.

3.5. N_2/Ar separation

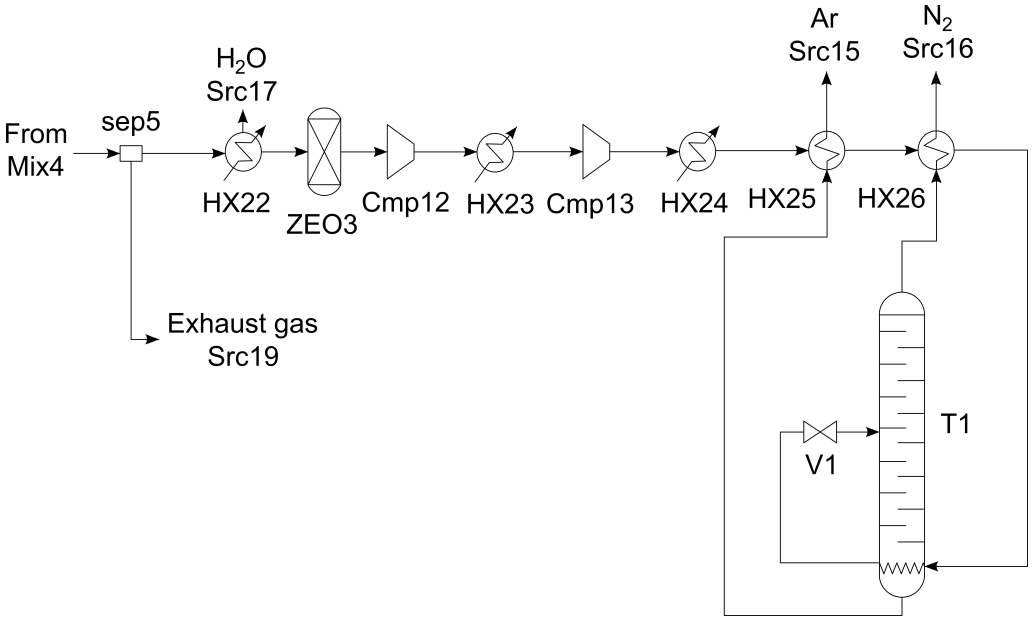

Figure 4: Process flow diagram for N_2/Ar separation section

The final gases, after the separation of hydrogen, contain mainly nitrogen and argon. On the one hand, nitrogen has been produced out of air for the synthesis of ammonia, and, in the case of power-to-ammonia, it has been previously obtained from different air separation technologies (Sánchez and Martín, 2018b). On the other hand, argon is fed into the ammonia combustion to limit the maximum temperature in the gas turbine.

Therefore, it is interesting to recover these two species. At this point, cryogenic distillation is proposed to separate them (as shown in Figure 4) following the schemes of air separation technologies. The first step is to compress the gases to a range of pressure between 40-60 bar. Then, the gases are cooled down providing the heat necessary in the reboiler of the distillation column. Finally, the gases are expanded up to ambient pressure, reducing the temperature and obtaining a biphasic stream that is introduced into the distillation column. To capture the thermodynamics of this system, difficult to model with simple equations, surrogate models have been developed to calculate the Joule-Thompson coefficient of the valve and the vapor fraction in the outlet stream. The rigorous models were developed in CHEMCAD 7.0 using the PRSK thermodynamic model. The following two polynomial regression models have been generated:

$$JT = -0.54978 + 0.01845T_{in} - 0.01676P_{in} \tag{9}$$

$$f_{vapor} = -1.13843 + 0.01432T_{in} - 0.00207P_{in} \tag{10}$$

Finally, after the valve, the gases are introduced into the cryogenic distillation column where the separation takes place. A recovery yield equal to 99.9% for nitrogen and 0.1% for argon in the top stream is fixed according to the results of the simulation of this system in CHEMCAD 7.0. Apart from the cryogenic distillation, it is also possible to release the gases without separation. In this case, it is not necessary to install the separation system, but argon and nitrogen are lost.

4. Solution Procedure

The design of an ammonia-to-power facility is formulated as a mixed-integer nonlinear programming (MINLP) problem to select the technologies and operating conditions that allow to produce. Six binary variables are present in the problem to determine whether or not to remove nitrogen oxides, the technology to recover the hydrogen and, finally, whether to introduce a step for the nitrogen/argon separation. The original MINLP problem is decomposed and eight nonlinear programming (NLP) problems are solved, one per possible combination of the binary variables. As objective function, a simplified operating cost for the production of power is used as follows:

$$obj = \sum_{i \epsilon IN} f_i C_i - \sum_{j \epsilon OUT} f_j C_j \tag{11}$$

where f_i is the inlet flow of each of the inlet/outlet resources and C_i its cost. The optimization problem is solved to minimize this simplified operating cost for a given power

demand. The ammonia cost is set to 0.5 €/kg (Pfromm, 2017), 0.037 €/kg for N_2 (Elishav et al., 2017), 0.5 €/kg for Ar (Downie, 2007) and 4 €/kg for H_2 (Matzen et al., 2015).

The problem is implemented in GAMS and solved using a multistart optimization approach using CONOPT 3.0 as the preferred solver. The size of the problem is approximately 1500-2000 equations and variables for each of the cases. After the optimization, an economic analysis is performed based on the methodology proposed by Sinnott (2014). Further details on the economic analysis methodology are provided in Table S1 of the Supporting Information. During the scale-up analysis, some of the units involved must be duplicated because the maximum level is reached. This behavior is included during the economic evaluation of the process.

5. Results

5.1. Main operating variables

In this section, a brief description of the main operating variables of the ammonia-to-power facility is presented. The value of these operating variables has been determined during the optimization procedure. In Table 1, a summary of the main results is shown when 100 MW is fixed as power capacity. In the ammonia decomposition section, the operating conditions of the reactor are the same regardless of the alternative: a temperature equal to 700 K, pressure to 10 bar and a gas inlet velocity of 1.5 m/s. With these conditions, a reactor conversion of more than 97% and a total recovery of hydrogen of more than 85% is reached. The temperature and pressure of the reactor are fixed to the minimum level allowed in the optimization problem. The lowest temperature is selected because the thermal energy to increase this variable is obtained from the outlet gases of the gas turbine. Therefore, if the thermal energy is used to heat up this stream, lower power generation is obtained. The minimum pressure is selected due to the cost of compression. If the inlet stream of the reactor is at a higher pressure, lower levels of power production are achieved in the facility, decreasing the energy efficiency.

For the preparation of the fuel blend, ammonia, hydrogen (produced from ammonia decomposition), argon and air are mixed. The flows of each feedstock in the facility are presented in Table 1. The inlet and outlet flows of the gas turbine are shown in more detail in Table S2 of the Supplementary Information. As a general trend, when the N_2/Ar separation is introduced to recycle both chemicals, a higher flow of ammonia is required. The reason for this is that the separation requires power to compress the gases before the cryogenic distillation and, since the plant is autonomous, the power must be produced within the plant, and, therefore, more fuel is needed. The performance of the gas turbine also determines the inlet flows of the components. The equivalent ratio (ER) is set to 1.2, if the gases are released into the atmosphere, or 1.4, if the N_2 and Ar are

Table 1: Main operating variables for the different alternatives: **A** - No SCR+Comb+N_2/Ar separation; **B** - No SCR+Comb+No N_2/Ar separation; **C**- No SCR+Mem+N_2/Ar separation; **D**- No SCR+Mem+No N_2/Ar separation; **E**- SCR+Comb+ N_2/Ar separation; **F**- SCR+Comb+No N_2/Ar separation; **G**- SCR+Mem+N_2/Ar separation; **H**-SCR+Mem+No N_2/Ar separation; **I** - No SCR+Mem without temperature limitation

		A	**B**	**C**	**D**	**E**	**F**	**G**	**H**	**I**
Power	Capacity (MW)	100	100	100	100	100	100	100	100	100
Inlet flows	Ammonia (kg/s)	17.79	14.74	15.83	13.31	17.86	14.74	15.97	13.30	11.07
	Air (kg/s)	88.68	64.07	92.22	75.13	88.20	64.07	92.65	75.10	64.85
	Ar (kg/s)	74.66	34.39	67.04	32.68	73.06	34.39	67.36	32.66	-
Ammonia Decomposition	Inlet T (K)	700	700	700	700	700	700	700	700	700
	Inlet P (bar)	10	10	10	10	10	10	10	10	10
	Inlet v (m/s)	1.5	1.5	1.5	1.5	1.5	1.5	1.5	1.5	0.85
Gas Turbine	Inlet P (bar)	8.41	6.00	6.80	6.90	8.49	6.00	6.30	6.93	12.26
	Combustion T (K)	1873	1873	1873	1873	1873	1873	1873	1873	2340
	Power (MW)	179.5	105.8	171.0	131.7	178.6	105.8	169.9	131.9	131.5
	ER	1.2	1.4	1.2	1.4	1.2	1.4	1.2	1.4	1.2
Steam Turbine	P high (bar)	125	125	125	125	125	125	125	125	125
	P inter (bar)	35	35	35	35	35	35	35	35	35
	P low (bar)	5	9.5	9.5	9.5	5	9.5	9.5	5	9.5
	T high (K)	782.0	991.6	785.9	785.9	782.8	991.6	785.9	782.8	785.9
	T inter (K)	564.0	745.7	567.1	567.1	564.0	745.7	567.1	564.0	567.1
	T low (K)	425.5	621.6	451.3	451.3	425.5	621.6	451.3	425.5	451.3
N_2/Ar Separation	P compr (bar)	40	-	40	-	40	-	40	-	-
	Inlet T (K)	77.13	-	77.26	-	77.42	-	77.30	-	-

separated. This is because, when the gases are discharged, the environmental restrictions must be met in terms of NO_x emissions. And, according to equation 7, following experimental results, these emissions increase when the ER decreases. Therefore, in order to comply with the maximum emission values, the ER must be reduced. The temperature of the combustion of the fuel blend is the same for all the alternatives 1873 K, limited by the upper limit for this temperature. If this constraint is relaxed, better performance in the gas turbine is expected and the introduction of argon as an inert could be avoided. In case **I** in Table 1, the scenario in which the temperature limitation is removed is presented. It is not necessary to introduce argon and, therefore, its separation using cryogenic distillation is also avoided, reducing considerably the capital and operating cost of the process. The maximum temperature in the gas turbine reaches 2340 K, allowing the same power generation with a small amount of inlet ammonia.

In the steam turbine, the maximum pressure value for each stage is reached, except for the value of the low-pressure turbine where the pressure range is between 5-9.5 bar. Also, as expected, higher inlet temperatures are obtained when combustion is introduced in the H_2 separation. More details about the conditions of the steam turbines are collected in Table S3 of the Supplementary Information. Finally, in the N_2/Ar separation unit, the gases are compressed up to 40 bar (the minimum level to avoid compression work) and the inlet temperature in the column is about 77 K.

5.2. Energy Efficiency

At this point, it is also interesting to evaluate the energy performance of the ammonia-to-power process. First of all, in Figure 5, a Sankey diagram is presented where the different energy flows are shown. The figure presents the best case in economic terms where no SCR treatment is included, H_2 is recovered by means of membranes and the N_2/Ar separation is included (case B in Table 1). The total energy involved in the main sections of the superstructure is presented in green boxes and the blue boxes represent the main products of the facility. The major input to the system is ammonia which is introduced into the fuel preparation section. This ammonia is mixed with the recycled hydrogen from the gas clean-up section to form the fuel of the combined cycle. Around 80% of the energy in the fuel blend comes from inlet ammonia. This fuel is fed to the power generation section. About 45% of the energy is transformed into power in the gas and steam turbines and approximately 30% of the total energy of the fuel remains in the flue gases. A fraction of the energy lost with the flue gases is recovered using the membranes that recycle the hydrogen to the fuel preparation section.

The energy efficiency of the process transformation is calculated as the ratio between the total power that is produced versus the heating value (LHV) of ammonia (as shown in equation 12):

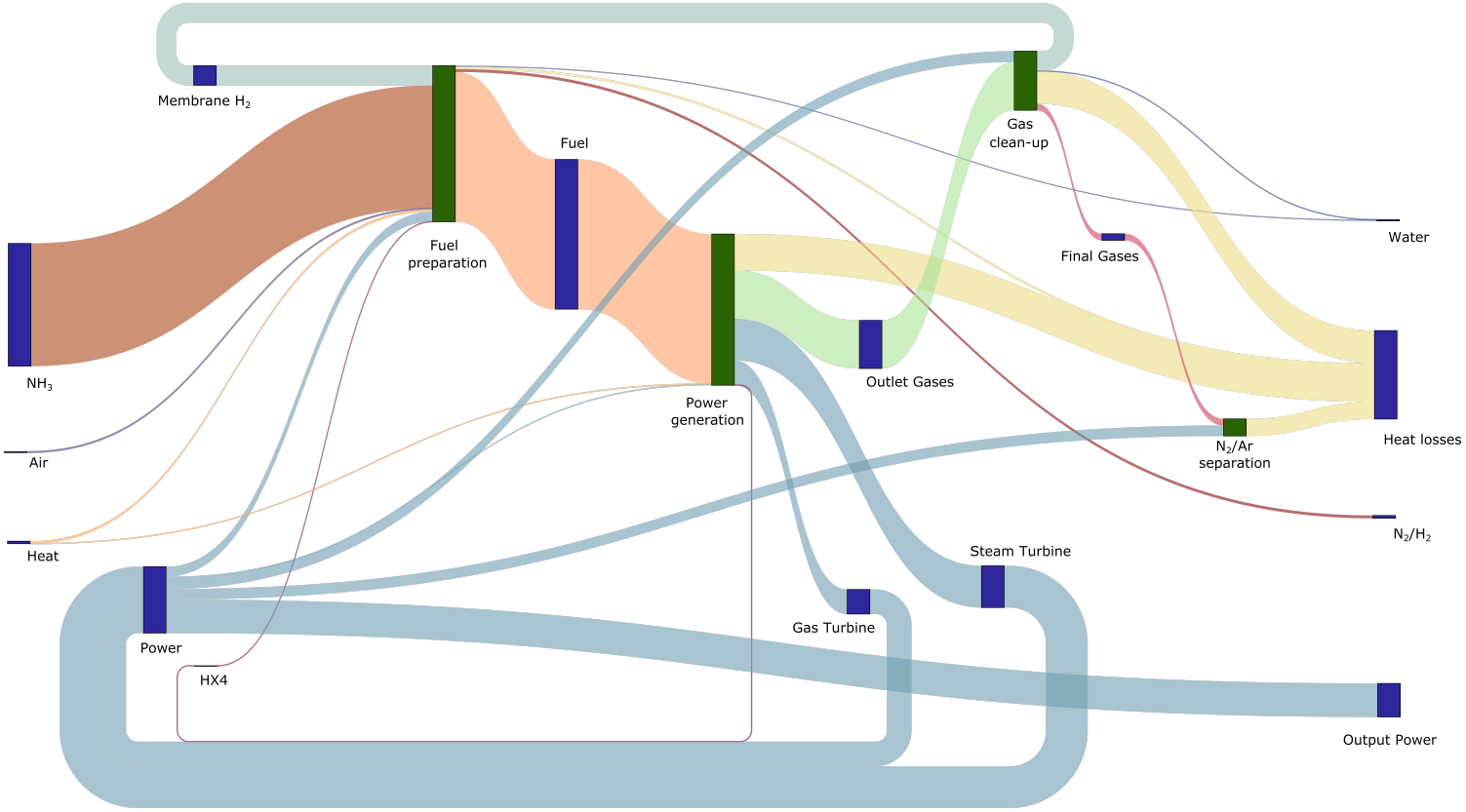

Figure 5: Sankey diagram for the flows of energy in the ammonia-to-power facility. The blue boxes represent the main products of the process and the green ones the total energy involved in the four main sections of the facility: fuel preparation, power generation, gas clean-up and N_2/Ar separation

$$\eta = \frac{W_{output}}{\dot{m}_{NH_3} LHV} 100 \tag{12}$$

The energy efficiencies for each of the evaluated alternatives in the ammonia-to-power superstructure are presented in Table 2.

Table 2: Energy efficiencies for the ammonia-to-power processes for a given capacity equal to 100 MW

	Process alternative	η (%)
A	No SCR+Comb+N_2/Ar separation	30.2
B	No SCR+Comb+No N_2/Ar separation	36.5
C	No SCR+Mem+N_2/Ar separation	34.0
D	No SCR+Mem+No N_2/Ar separation	40.4
E	SCR+Comb+N_2/Ar separation	30.1
F	SCR+Comb+No N_2/Ar separation	36.5
G	SCR+Mem+N_2/Ar separation	33.7
H	SCR+Mem+No N_2/Ar separation	40.4
I	No SCR+Mem without temperature limitation	48.6

The efficiency of the process alternatives that use membranes is higher than those that burn hydrogen (2-3% higher efficiency). In addition, the introduction of N_2/Ar separation reduces the energy efficiency of the process, by around 15%. This is due to the fact that the separation involves energy consumption that must be provided using the power produced in the facility. Therefore, the total production of power is lower. At this point, based only on energy efficiencies, the use of N_2/Ar separation is detrimental to the performance of the process. Nevertheless, the economic implications of these decisions are evaluated in the following section. If the temperature constraint is relaxed, a maximum efficiency of almost 50% is achieved in the ammonia-to-power transformation. Therefore, an enhanced design for the gas turbines can help improve the energy efficiency of the process. These results are consistent with respect to previous analysis. Božo and Valera-Medina (2020) studied the operation of a humidified gas turbine alone excluding the combined cycle, the preparation of raw materials and the gas-clean up section. The maximum efficiency of this system was 43.4%. Keller et al. (2020) carried out a thermodynamic analysis of a combined cycle, including only the gas and steam turbines. The maximum efficiency in that work increased to about 60%. Therefore, the introduction of the Rankine cycle improves the energy performance of the ammonia-to-power transformation, and the introduction of all the sections of the facility is required to obtain an accurate efficiency of the power generation from ammonia. It is also interesting to compare the values of efficiency obtained in this work (as shown Table 2)

with those achieved from the ammonia fuel cells, the other main alternative in the use of ammonia for power production. Ezzat and Dincer (2020) computed the ammonia solid oxide fuel cell (SOFC) efficiency reaching values of about 65 %. Other studies reduce this value to about 45 % (Zhao et al., 2019). Therefore, the fuel cell systems may have slightly higher efficiencies than the thermo-chemical route. However, the fuel cells are developed, in general, for small-scale applications, for instance, vehicles. Thus, the thermo-chemical pathway could be appropriate for utility applications with higher power consumptions such as grid management. The value of the ammonia-to-power thermo-chemical efficiencies can also be put into perspective with the traditional power generation system. Coal-based power facilities have an efficiency of about 40 %, nuclear around 45 % or combined cycle using natural gas about 50 % (Suppes and Storvick, 2007). These values are similar those obtained using ammonia, demonstrating the great potential of this chemical as a carbon-free fuel.

5.3. Economic Analysis

An economic analysis of the different alternatives for transforming ammonia into power is presented in this section. Figure 6 represents the production and capital cost for the process alternatives where SCR technology is not included. Different capacities are evaluated in the figure for analyzing the influence of the scale on the profitability of the process including the modular behavior of some units. It is clear that alternatives where N_2/Ar separation is included reduce drastically the production cost of the power from about 0.9-1 €/kWh to 0.2-0.3 €/kWh. As Figure 6 shows, it is necessary to increase the investment to introduce this new section, however, the possibility of recycling the obtained gases to the ammonia synthesis and to the combustion zone justifies this increase. Furthermore, the introduction of this unit decreases the global efficiency of the transformation as the previous section explained. But, the better economic performance supports the addition of the separation. If the decision regarding the gas cleanup is analyzed (membrane versus combustion for the H_2 treatment), the use of membranes reduces the capital and operating costs of the facility. An increment of about 5% is expected when combustion is selected compared to membranes. Hydrogen is a valuable component and the preferred option is to recycle it to avoid the consumption of ammonia in the membrane reactor versus the option of using it to reheat the steam in the Rankine cycle.

Similarly, Figure 7 shows the production and capital cost when the SCR technology to remove the NO_x is introduced. As in the case where SCR is not included, the use of membranes for the recovery of hydrogen show better economic performance than the combustion of the gas stream as clean-up stage and the N_2/Ar separation significantly reduces the production cost of power. If the introduction of SCR technology is

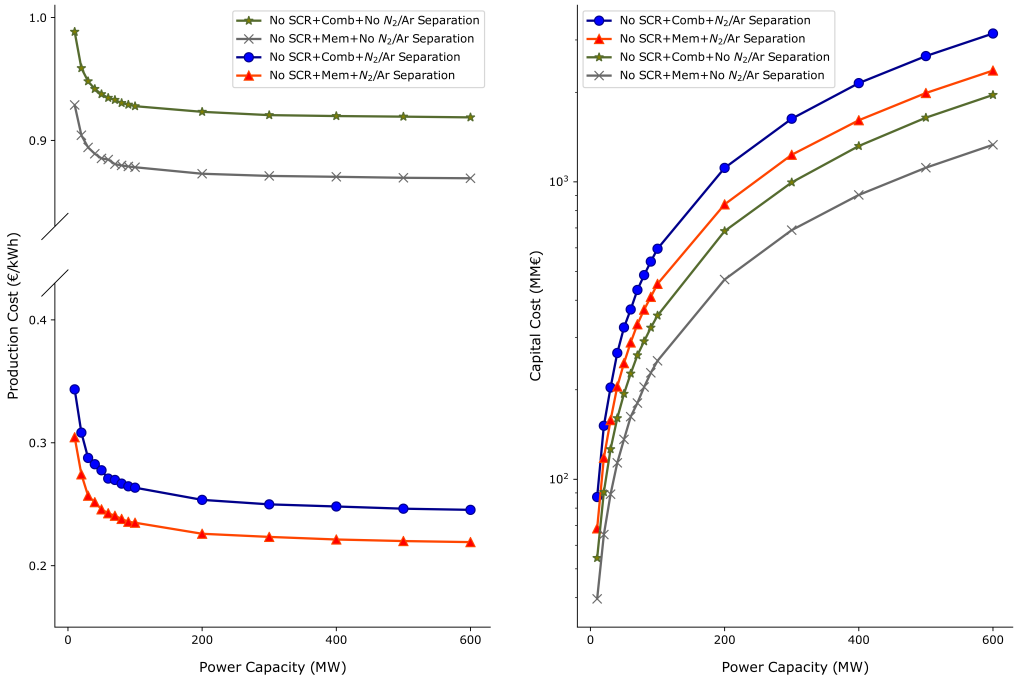

Figure 6: Capital and operating cost for the alternatives without SCR technology

evaluated, a logical increase in the production and capital cost takes place because the new treatment requires introducing a new unit. An increase of about 0.02-0.04 €/kWh is expected when SCR is selected. However, from a sustainable point of view, the introduction of this technology could be suitable to be able to produce CO_2-free power but also free of other pollutants such as nitrogen oxides. Consequently, this increment could be acceptable and assumed by society.

To summarize, the best alternative to carry out the ammonia-to-power transformation, from the economic standpoint, is the combination of membranes and the N_2/Ar separation excluding the SCR technology. In this case, a capital cost of about 450 MM€ and a production cost of 0.2 €/kWh is expected for a facility with a production capacity of 100 MW. If the SCR technology is included, in order to improve the sustainability of the process, the investment increase to about 550 MM€ with a production cost of 0.25 €/kWh.

Figure 8 shows the breakdown of the investment and production costs for the best alternatives, whether NO_x catalytic removal or not is implemented. This presents the two best alternatives, including or not selective catalytic removal. The heat exchangers are the main item in the distribution of the capital cost in both cases (Figure 8a and 8c)

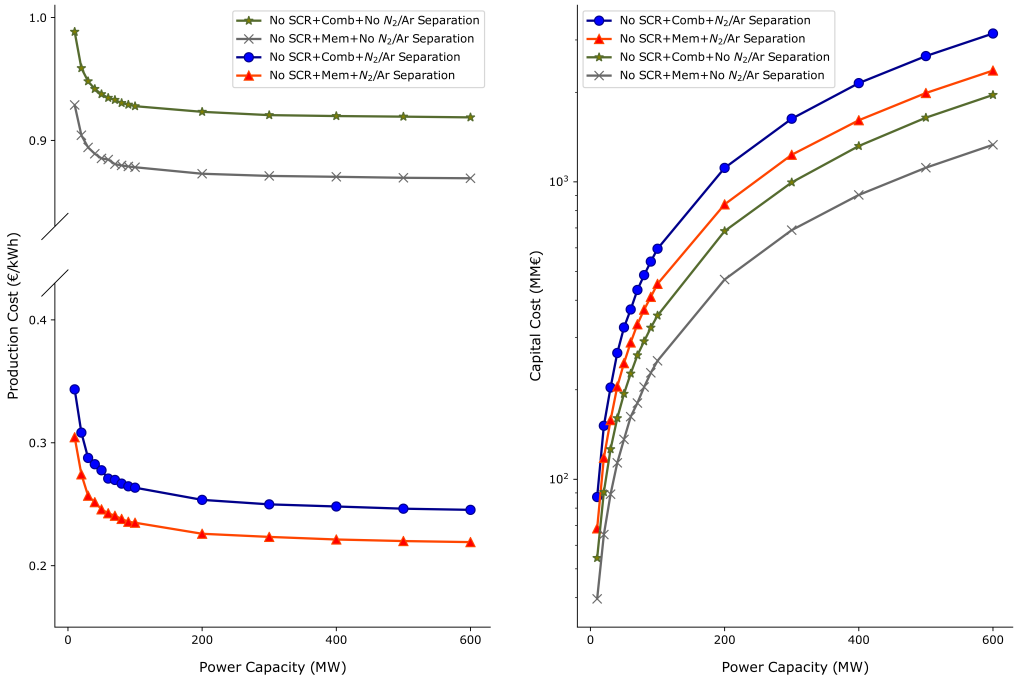

Figure 7: Capital and operating cost for the alternatives without SCR technology

with around 50% of the total inversion followed by the compressors. The NO_x treatment also represents an important percentage (≈ 20%) of the total capital cost when this technology is included in the ammonia-to-power process (Figure 8a). In the case of the operating costs, the raw materials are the most important element, with about 50% of the total production cost (Figure 8b and 8d). The capital charges are about 20-25%, representing a higher percentage when the SCR is included due to the increment of the capital cost for these new units. These results clearly show the crucial importance of the cost of ammonia in the profitability of these power generation facilities.

5.4. Sensitivity Analysis

Due to the central relevance of the price of ammonia in power generation, a sensitivity analysis is performed to assess the impact of the different ammonia prices in the power production cost. The price of green ammonia depends on the technology (power-to-ammonia (Sánchez and Martín, 2018a) or biomass gasification/digestion (Sánchez et al., 2019)) and a significant reduction is expected in the coming years, mainly, in the power-to-ammonia processes due to the reduction of the cost of PV panels and wind turbines and also in the electrolysis technologies. The influence of the ammonia price and the power production capacity in the power cost is presented in Figure 9.

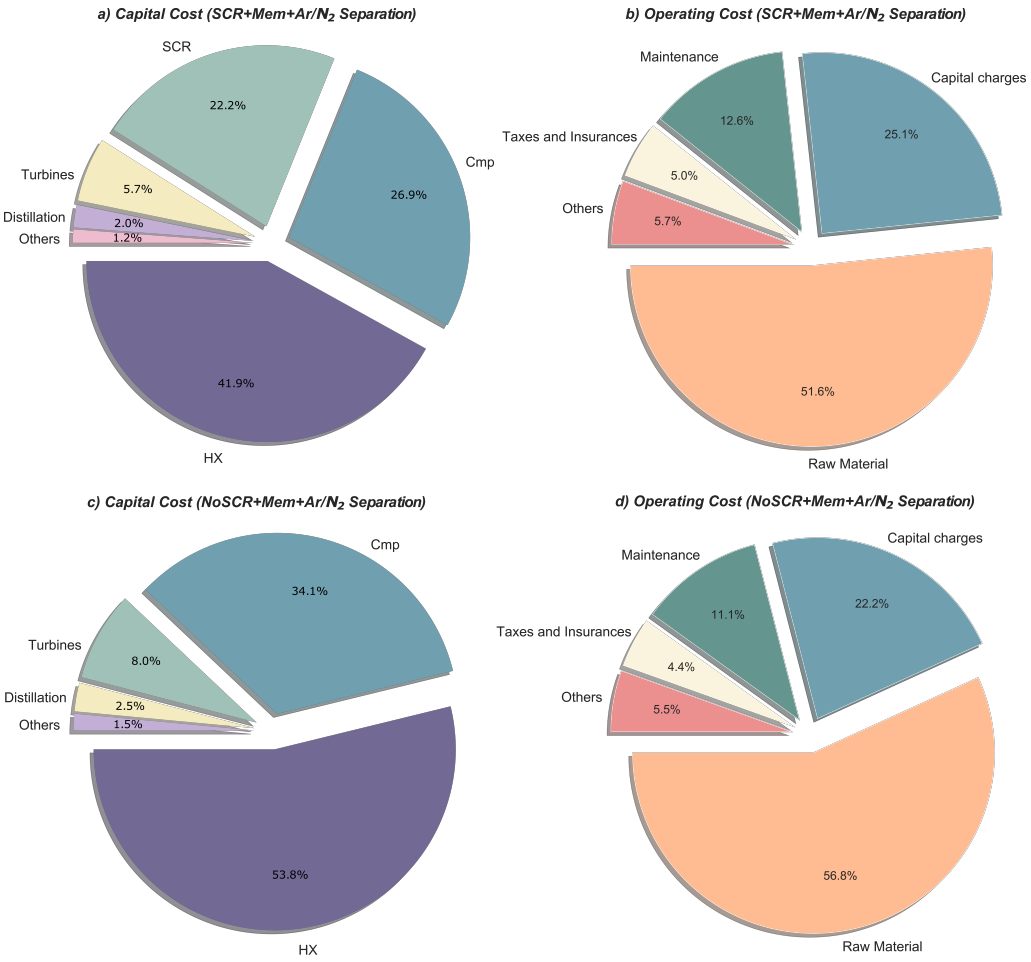

Figure 8: Breakdown of the capital and operating cost for the most promising technologies in the ammonia-to-power process

The ammonia price in the sensitivity analysis is in the range of 0.2-1.4 €/kg. Using these levels, it is possible to capture the current and expected prices of ammonia using renewable sources. The ongoing base prices levels are: ≈ 1.4 €/kg for power-to-ammonia using membranes for air separation, ≈ 1.3 €/kg using distillation, ≈ 1.2 €/kg for the PSA and about 0.4-0.6 €/kg for the biomass-based alternatives. The range for the power capacity is 10-600 MW.

With the current prices of ammonia, especially, power-to-ammonia alternatives, the production cost of power is about 0.5-0.8 €/kWh but a promising cost of about 0.2-0.4 €/kWh could be reached in the next years if the expected reduction in the ammonia prices comes true. For a better comparison, the cost of the ammonia-to-power is put

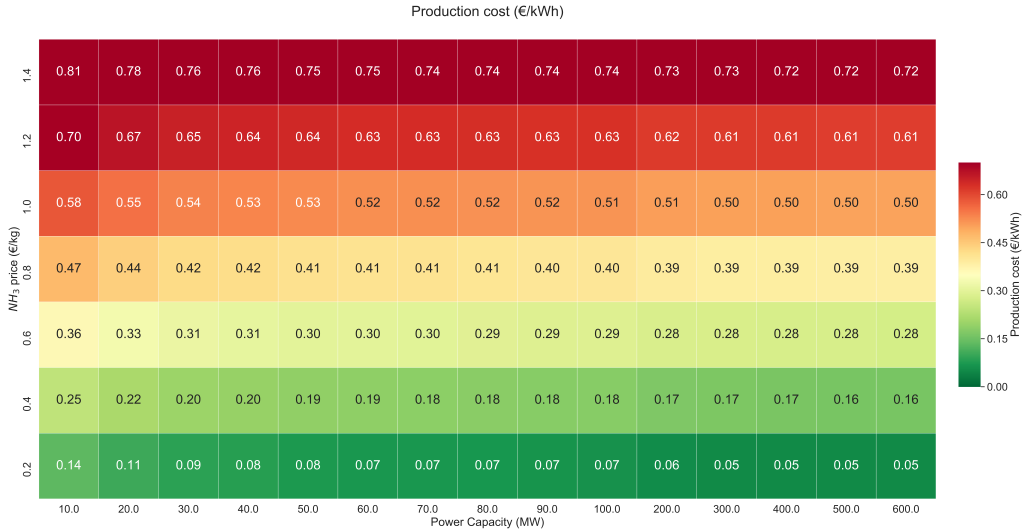

Figure 9: Effect of the ammonia price and the facility capacity in the power production cost

into perspective with the production cost of different renewable energy sources. For instance, the cost of power generation using PV panels is about 0.05-0.1 €/kWh, from wind turbines between 0.1-0.15 €/kWh or the biogas about 0.15 €/kWh (Kost et al., 2018). Note that power from PV panels or wind turbines is highly volatile while that based on ammonia can be stable over time. In other traditional sources, the cost of electricity is in the range of 0.05-0.1 €/kWh for coal facilities or up to 0.22 €/kWh in the case of gas-based power generation (Kost et al., 2018). As expected, storage alternatives are more expensive than direct power production. However, a range of 0.2-0.4 €/kWh for the ammonia-to-power process is competitive for introducing this technology into the power grid in order to increase its robustness. With these price levels, it is possible to create a competitive cost for electricity combining renewable sources and different energy storage technologies. And, by using the ammonia-to-power alternative, it is possible to provide a clean and carbon-free storage option for different time scales and capacities.

6. Conclusions

This work presents a process scale analysis for the ammonia-to-power transformation. Ammonia could be key in the future energy system as a carbon-free technology to store energy and, also, as an energy carrier. Therefore, the evaluation of the potential transformation of ammonia into power is critical for the possible uses of ammonia in the new sustainable energy paradigm. In this work, a mixture of ammonia/hydrogen

is used as fuel for the combined cycle. This hydrogen is produced through ammonia decomposition. In addition, different gas cleanup alternatives have been proposed including SCR NO_x removal, different H_2 recovery technologies and the final N_2/Ar separation. An equation-based optimization approach is developed to determine the optimal path and the conditions of ammonia-based power production. A technical and economic evaluation is presented for the different alternatives. The best alternative, in economic terms, in the ammonia-to-power transformation is the combination of membranes for hydrogen recovery and N_2/Ar separation with no treatment for nitrogen oxides removal. Energy efficiencies of around 40% are reached for the complete transformation of ammonia into power, including not only the gas turbine but also the entire process. The production cost ranges between 0.2-0.6 €/kWh, which could be competitive for the integration of this technology into a renewable energy scheme. Therefore, the potential of the use of ammonia as a fuel for energy storage is demonstrated in this work in a context where the high penetration of renewable energy sources required the implementation of the energy storage at grid scale. For the full deployment of the use of ammonia in the energy system, further analysis is needed regarding materials for ammonia gas turbines and the potential degradation. Moreover, an analysis including all the production and storage technologies at grid-scale is necessary to determine the contribution of each of these technologies towards the goal of achieving a 100% renewable energy system.

Nomenclature

a_i	Activity of component i (atm)
C_i	Cost of product i (€/kg)
ER	Equivalent ratio
f_{vapor}	vapor fraction
f_i	Total flow (kg/s)
JT	Joule-Thompson coefficient (K/bar)
L_{reac}	Length of the decomposition reactor (m)
LHV	Lower heating value (kJ/kg)
$\dot{m}_{NH_3}$	Inlet molar flow of ammonia (kg/s)
P	Pressure (atm)
P_i	Partial pressure of component i (atm)
k_{reac}	Rate constant (kmol/m^3 hr)
K_p	Equilibrium constant (1/atm)
r	Reaction rate (kmol/m^3 hr)

$r^p_{H_2}$	Permeation rate (kmol/m^2 hr)
T	Temperature (K)
v_{reac}	Inlet velocity of the gases (m/s)
W_{output}	Total power production (kJ)
X_{reac}	Conversion in the fixed bed
X_{total}	Total H_2 recovery in the membrane reactor
α	Kinetic parameter
β_i	Polynomial regression coefficient
δ	Thickness of the membrane (μm)
η	Energy efficiency
Ω	Catalytic activity
Φ	Effectiveness factor

Acknowledgments

The authors acknowledge MICINN Spain grant PID2019-105434RB-C31 and the FPU, Spain grant (FPU16/06212) to A.S.

References

Abashar, M., 2018. Ultra-clean hydrogen production by ammonia decomposition. Journal of King Saud University - Engineering Sciences 30, 2 – 11. URL: http://www.sciencedirect.com/science/article/pii/S1018363916000064, doi:https://doi.org/10.1016/j.jksues.2016.01.002.

Al-Qahtani, A., González-Garay, A., Bernardi, A., Galán-Martín, A., Pozo, C., Dowell, N.M., Chachuat, B., Guillén-Gosálbez, G., 2020. Electricity grid decarbonisation or green methanol fuel? a life-cycle modelling and analysis of todays transportation-power nexus. Applied Energy 265, 114718. URL: http://www.sciencedirect.com/science/article/pii/S0306261920302300, doi:https://doi.org/10.1016/j.apenergy.2020.114718.

Allman, A., Daoutidis, P., 2018. Optimal scheduling for wind-powered ammonia generation: Effects of key design parameters. Chemical Engineering Research and Design 131, 5 – 15. URL: http://www.sciencedirect.com/science/article/pii/S0263876217305646, doi:https://doi.org/10.1016/j.cherd.2017.10.010. energy Systems Engineering.

BloombergNEF, 2020. New energy outlook 2020. URL: https://about.bnef.com/new-energy-outlook/.

Božo, M.G., Valera-Medina, A., 2020. Prediction of novel humified gas turbine cycle parameters for ammonia/hydrogen fuels. Energies 13, 5749.

Cesaro, Z., Ives, M., Nayak-Luke, R., Mason, M., Bañares-Alcántara, R., 2021. Ammonia to power: Forecasting the levelized cost of electricity from green ammonia in large-scale power plants. Applied Energy 282, 116009. URL: http://www.sciencedirect.com/science/article/pii/S0306261920314549, doi:https://doi.org/10.1016/j.apenergy.2020.116009.

Child, M., Kemfert, C., Bogdanov, D., Breyer, C., 2019. Flexible electricity generation, grid exchange and storage for the transition to a 100% renewable energy system in europe. Renewable Energy 139, 80 – 101. URL: http://www.sciencedirect.com/science/article/pii/S0960148119302319, doi:https://doi.org/10.1016/j.renene.2019.02.077.

Chiuta, S., Everson, R.C., Neomagus, H.W., van der Gryp, P., Bessarabov, D.G., 2013. Reactor technology options for distributed hydrogen generation via ammonia decomposition: A review. International Journal of Hydrogen Energy 38, 14968 – 14991. URL: http://www.sciencedirect.com/science/article/pii/S0360319913022908, doi:https://doi.org/10.1016/j.ijhydene.2013.09.067.

Daggash, H.A., Patzschke, C.F., Heuberger, C.F., Zhu, L., Hellgardt, K., Fennell, P.S., Bhave, A.N., Bardow, A., Mac Dowell, N., 2018. Closing the carbon cycle to maximise climate change mitigation: power-to-methanol vs. power-to-direct air capture. Sustainable Energy Fuels 2, 1153–1169. URL: http://dx.doi.org/10.1039/C8SE00061A, doi:10.1039/C8SE00061A.

Davis, W., Martín, M., 2014. Optimal year-round operation for methane production from co2 and water using wind and/or solar energy. Journal of Cleaner Production 80, 252 – 261. URL: http://www.sciencedirect.com/science/article/pii/S0959652614005563, doi:https://doi.org/10.1016/j.jclepro.2014.05.077.

De Falco, M., Marrelli, L., Iaquaniello, G., 2011. Membrane reactors for hydrogen production processes .

Di Sarli, V., Cammarota, F., Salzano, E., Di Benedetto, A., 2017. Explosion behavior of ammonia and ammonia/methane in oxygen-enriched air. Process Safety Progress 36, 368–371. URL: https://aiche.onlinelibrary.wiley.com/doi/abs/10.1002/prs.11912, doi:https://doi.org/10.1002/prs.11912, arXiv:https://aiche.onlinelibrary.wiley.com/doi/pdf/10.1002/prs.11912.

Dieterich, V., Buttler, A., Hanel, A., Spliethoff, H., Fendt, S., 2020. Power-to-liquid via synthesis of methanol, dme or fischer–tropsch-fuels: a review. Energy Environ. Sci. 13, 3207–3252. URL: http://dx.doi.org/10.1039/D0EE01187H, doi:10.1039/D0EE01187H.

Downie, N.A., 2007. Industrial gases. Springer Science & Business Media.

Ehrenstein, M., Ángel Galán-Martín, Tulus, V., Guillén-Gosálbez, G., 2020. Optimising fuel supply chains within planetary boundaries: A case study of hydrogen for road transport in the uk. Applied Energy 276, 115486. URL: http://www.sciencedirect.com/science/article/pii/S0306261920309983, doi:https://doi.org/10.1016/j.apenergy.2020.115486.

Elishav, O., Tvil, G., Mosevitzky, B., Lewin, D., Shter, G.E., Grader, G.S., 2017. The nitrogen economy: The feasibility of using nitrogen-based alternative fuels. Energy Procedia 135, 3 – 13. URL: http://www.sciencedirect.com/science/article/pii/S187661021734585X, doi:https://doi.org/10.1016/j.egypro.2017.09.482. 11th International Renewable Energy Storage Conference, IRES 2017, 14-16 March 2017, Düsseldorf, Germany.

European Commission, 2020. A hydrogen strategy for a climate-neutral europe .

European Council, 2010. Directive 2010/75/eu of the european parliament and of the council. Off. J. Eur. Union L 334, 17–119.

Ezzat, M., Dincer, I., 2020. Energy and exergy analyses of a novel ammonia combined power plant operating with gas turbine and solid oxide fuel cell systems. Energy 194, 116750. URL: http://www.sciencedirect.com/science/article/pii/S0360544219324454, doi:https://doi.org/10.1016/j.energy.2019.116750.

Fúnez Guerra, C., Reyes-Bozo, L., Vyhmeister, E., Jaén Caparrós, M., Salazar, J.L., Clemente-Jul, C., 2020. Technical-economic analysis for a green ammonia production plant in chile and its subsequent transport to japan. Renewable Energy 157, 404 – 414. URL: http://www.sciencedirect.com/science/article/pii/S0960148120307394, doi:https://doi.org/10.1016/j.renene.2020.05.041.

Frate, G.F., Ferrari, L., Desideri, U., 2021. Energy storage for grid-scale applications: Technology review and economic feasibility analysis. Renewable Energy 163, 1754 – 1772. URL: http://www.sciencedirect.com/science/article/pii/S0960148120316360, doi:https://doi.org/10.1016/j.renene.2020.10.070.

Gür, T.M., 2018. Review of electrical energy storage technologies, materials and systems: challenges and

prospects for large-scale grid storage. Energy Environ. Sci. 11, 2696–2767. URL: http://dx.doi.org/10.1039/C8EE01419A, doi:10.1039/C8EE01419A.

Götz, M., Lefebvre, J., Mörs, F., McDaniel Koch, A., Graf, F., Bajohr, S., Reimert, R., Kolb, T., 2016. Renewable power-to-gas: A technological and economic review. Renewable Energy 85, 1371 – 1390. URL: http://www.sciencedirect.com/science/article/pii/S0960148115301610, doi:https://doi.org/10.1016/j.renene.2015.07.066.

Gu, C.w., Wang, H., Ji, X.x., Li, X.s., 2016. Development and application of a thermodynamic-cycle performance analysis method of a three-shaft gas turbine. Energy 112, 307 – 321. URL: http://www.sciencedirect.com/science/article/pii/S0360544216308684, doi:https://doi.org/10.1016/j.energy.2016.06.094.

Guerras, L.S., Martín, M., 2019. Optimal gas treatment and coal blending for reduced emissions in power plants: A case study in northwest spain. Energy 169, 739 – 749. URL: http://www.sciencedirect.com/science/article/pii/S0360544218324551, doi:https://doi.org/10.1016/j.energy.2018.12.089.

Heras, J., Martín, M., 2021. Multiscale analysis for power-to-gas-to-power facilities based on energy storage. Computers & Chemical Engineering 144, 107147. URL: http://www.sciencedirect.com/science/article/pii/S009813542030853X, doi:https://doi.org/10.1016/j.compchemeng.2020.107147.

Jeerh, G., Zhang, M., Tao, S., 2021. Recent progress in ammonia fuel cells and their potential applications. J. Mater. Chem. A 9, 727–752. URL: http://dx.doi.org/10.1039/D0TA08810B, doi:10.1039/D0TA08810B.

Jo, Y.S., Cha, J., Lee, C.H., Jeong, H., Yoon, C.W., Nam, S.W., Han, J., 2018. A viable membrane reactor option for sustainable hydrogen production from ammonia. Journal of Power Sources 400, 518 – 526. URL: http://www.sciencedirect.com/science/article/pii/S0378775318308693, doi:https://doi.org/10.1016/j.jpowsour.2018.08.010.

Keller, M., Koshi, M., Otomo, J., Iwasaki, H., Mitsumori, T., Yamada, K., 2020. Thermodynamic evaluation of an ammonia-fueled combined-cycle gas turbine process operated under fuel-rich conditions. Energy 194, 116894. URL: http://www.sciencedirect.com/science/article/pii/S0360544220300013, doi:https://doi.org/10.1016/j.energy.2020.116894.

Khateeb, A.A., Guiberti, T.F., Zhu, X., Younes, M., Jamal, A., Roberts, W.L., 2020. Stability limits and no emissions of technically-premixed ammonia-hydrogen-nitrogen-air swirl flames. International Journal of Hydrogen Energy 45, 22008 – 22018. URL: http://www.sciencedirect.com/science/article/pii/S0360319920320917, doi:https://doi.org/10.1016/j.ijhydene.2020.05.236.

Kim, S., Song, J., Lim, H., 2018. Conceptual feasibility studies of a co x-free hydrogen production from ammonia decomposition in a membrane reactor for pem fuel cells. Korean Journal of Chemical Engineering 35, 1509–1516.

Kobayashi, H., Hayakawa, A., Somarathne, K.K.A., Okafor, E.C., 2019. Science and technology of ammonia combustion. Proceedings of the Combustion Institute 37, 109 – 133. URL: http://www.sciencedirect.com/science/article/pii/S1540748918306345, doi:https://doi.org/10.1016/j.proci.2018.09.029.

Kost, C., Shammugam, S., Jülch, V., Nguyen, H.T., Schlegl, T., 2018. Levelized cost of electricity renewable energy technologies. Fraunhofer Institute for Solar Energy Systems ISE .

León, E., Martín, M., 2016. Optimal production of power in a combined cycle from manure based biogas. Energy Conversion and Management 114, 89 – 99. URL: http://www.sciencedirect.com/science/article/pii/S0196890416300255, doi:https://doi.org/10.1016/j.enconman.2016.02.002.

Li, G., Kanezashi, M., Yoshioka, T., Tsuru, T., 2013. Ammonia decomposition

in catalytic membrane reactors: Simulation and experimental studies. AIChE Journal 59, 168–179. URL: https://aiche.onlinelibrary.wiley.com/doi/abs/10.1002/aic.13794, doi:https://doi.org/10.1002/aic.13794, arXiv:https://aiche.onlinelibrary.wiley.com/doi/pdf/10.1002/aic.13794.

MacFarlane, D.R., Cherepanov, P.V., Choi, J., Suryanto, B.H., Hodgetts, R.Y., Bakker, J.M., Ferrero Vallana, F.M., Simonov, A.N., 2020. A roadmap to the ammonia economy. Joule 4, 1186–1205. URL: https://www.sciencedirect.com/science/article/pii/S2542435120301732, doi:https://doi.org/10.1016/j.joule.2020.04.004.

Martín, M., 2016. Optimal year-round production of dme from co2 and water using renewable energy. Journal of CO2 Utilization 13, 105 – 113. URL: http://www.sciencedirect.com/science/article/pii/S2212982016300038, doi:https://doi.org/10.1016/j.jcou.2016.01.003.

Matzen, M., Alhajji, M., Demirel, Y., 2015. Chemical storage of wind energy by renewable methanol production: Feasibility analysis using a multi-criteria decision matrix. Energy 93, 343 – 353. URL: http://www.sciencedirect.com/science/article/pii/S0360544215012530, doi:https://doi.org/10.1016/j.energy.2015.09.043.

Meroueh, L., Chen, G., 2020. Thermal energy storage radiatively coupled to a supercritical rankine cycle for electric grid support. Renewable Energy 145, 604 – 621. URL: http://www.sciencedirect.com/science/article/pii/S0960148119308584, doi:https://doi.org/10.1016/j.renene.2019.06.036.

Mohammadi, A., Mehrpooya, M., 2018. A comprehensive review on coupling different types of electrolyzer to renewable energy sources. Energy 158, 632 – 655. URL: http://www.sciencedirect.com/science/article/pii/S0360544218311381, doi:https://doi.org/10.1016/j.energy.2018.06.073.

Mounaïm-Rousselle, C., Brequigny, P., 2020. Ammonia as fuel for low-carbon spark-ignition engines of tomorrow's passenger cars. Frontiers in Mechanical Engineering 6, 70. URL: https://www.frontiersin.org/article/10.3389/fmech.2020.00070, doi:10.3389/fmech.2020.00070.

Otomo, J., Koshi, M., Mitsumori, T., Iwasaki, H., Yamada, K., 2018. Chemical kinetic modeling of ammonia oxidation with improved reaction mechanism for ammonia/air and ammonia/hydrogen/air combustion. International Journal of Hydrogen Energy 43, 3004 – 3014. URL: http://www.sciencedirect.com/science/article/pii/S0360319917347055, doi:https://doi.org/10.1016/j.ijhydene.2017.12.066.

Paixão, V.P., Secchi, A.R., Melo, P.A., 2018. Preliminary design of a municipal solid waste biorefinery for environmentally friendly nh3 production. Industrial & Engineering Chemistry Research 57, 15437–15449. URL: https://doi.org/10.1021/acs.iecr.8b02927, doi:10.1021/acs.iecr.8b02927, arXiv:https://doi.org/10.1021/acs.iecr.8b02927.

Palys, M.J., Wang, H., Zhang, Q., Daoutidis, P., 2021. Renewable ammonia for sustainable energy and agriculture: vision and systems engineering opportunities. Current Opinion in Chemical Engineering 31, 100667. URL: http://www.sciencedirect.com/science/article/pii/S2211339820300708, doi:https://doi.org/10.1016/j.coche.2020.100667.

Pellow, M.A., Emmott, C.J.M., Barnhart, C.J., Benson, S.M., 2015. Hydrogen or batteries for grid storage? a net energy analysis. Energy Environ. Sci. 8, 1938–1952. URL: http://dx.doi.org/10.1039/C4EE04041D, doi:10.1039/C4EE04041D.

Pfromm, P.H., 2017. Towards sustainable agriculture: Fossil-free ammonia. Journal of Renewable and Sustainable Energy 9, 034702.

van Renssen, S., 2020. The hydrogen solution? Nature Climate Change 10, 799–801.

Resitoglu, I.A., Keskin, A., 2017. Hydrogen applications in selective catalytic reduction of nox emissions from diesel engines. International Journal of Hydrogen Energy 42, 23389 – 23394. URL: http://www.sciencedirect.com/science/article/pii/S0360319917304275, doi:https://doi.org/10.

1016/j.ijhydene.2017.02.011.

Sadi, M., Arabkoohsar, A., 2019. Exergoeconomic analysis of a combined solar-waste driven power plant. Renewable Energy 141, 883 – 893. URL: http://www.sciencedirect.com/science/article/pii/S0960148119305543, doi:https://doi.org/10.1016/j.renene.2019.04.070.

Siddiqui, O., Dincer, I., 2020. Experimental investigation of a sustainable integrated ammonia synthesis and fuel cell system. Fuel 278, 118300. URL: http://www.sciencedirect.com/science/article/pii/S0016236120312965, doi:https://doi.org/10.1016/j.fuel.2020.118300.

Siddiqui, O., Ishaq, H., Dincer, I., 2020. Experimental investigation of improvement capability of ammonia fuel cell performance with addition of hydrogen. Energy Conversion and Management 205, 112372. URL: http://www.sciencedirect.com/science/article/pii/S0196890419313792, doi:https://doi.org/10.1016/j.enconman.2019.112372.

Sinnott, R., 2014. Chemical engineering design. volume 6. Elsevier.

Sánchez, A., Hernández, B., Martín, M., 2020. Multiscale Analysis for the Exploitation of Bioresources. John Wiley and Sons, Ltd. chapter 3. pp. 49–83. URL: https://onlinelibrary.wiley.com/doi/abs/10.1002/9781119582694.ch3, doi:https://doi.org/10.1002/9781119582694.ch3, arXiv:https://onlinelibrary.wiley.com/doi/pdf/10.1002/9781119582694.ch3.

Sánchez, A., Martín, M., 2018a. Optimal renewable production of ammonia from water and air. Journal of Cleaner Production 178, 325 – 342. URL: http://www.sciencedirect.com/science/article/pii/S0959652617332730, doi:https://doi.org/10.1016/j.jclepro.2017.12.279.

Sánchez, A., Martín, M., 2018b. Scale up and scale down issues of renewable ammonia plants: Towards modular design. Sustainable Production and Consumption 16, 176 – 192. URL: http://www.sciencedirect.com/science/article/pii/S2352550918300812, doi:https://doi.org/10.1016/j.spc.2018.08.001.

Sánchez, A., Martín, M., Vega, P., 2019. Biomass based sustainable ammonia production: Digestion vs gasification. ACS Sustainable Chemistry & Engineering 7, 9995–10007. URL: https://doi.org/10.1021/acssuschemeng.9b01158, doi:10.1021/acssuschemeng.9b01158, arXiv:https://doi.org/10.1021/acssuschemeng.9b01158.

Sternberg, A., Bardow, A., 2016. Life cycle assessment of power-to-gas: Syngas vs methane. ACS Sustainable Chemistry & Engineering 4, 4156–4165. URL: https://doi.org/10.1021/acssuschemeng.6b00644, doi:10.1021/acssuschemeng.6b00644, arXiv:https://doi.org/10.1021/acssuschemeng.6b00644.

Suppes, G.J., Storvick, T., 2007. Sustainable nuclear power. Elsevier.

UN General Assembly, 2015. Transforming our world: the 2030 agenda for sustainable development. Division for Sustainable Development Goals: New York, NY, USA .

Valera-Medina, A., Gutesa, M., Xiao, H., Pugh, D., Giles, A., Goktepe, B., Marsh, R., Bowen, P., 2019. Premixed ammonia/hydrogen swirl combustion under rich fuel conditions for gas turbines operation. International Journal of Hydrogen Energy 44, 8615 – 8626. URL: http://www.sciencedirect.com/science/article/pii/S0360319919305907, doi:https://doi.org/10.1016/j.ijhydene.2019.02.041.

Valera-Medina, A., Marsh, R., Runyon, J., Pugh, D., Beasley, P., Hughes, T., Bowen, P., 2017. Ammonia–methane combustion in tangential swirl burners for gas turbine power generation. Applied Energy 185, 1362 – 1371. URL: http://www.sciencedirect.com/science/article/pii/S0306261916302100, doi:https://doi.org/10.1016/j.apenergy.2016.02.073. clean, Efficient and Affordable Energy for a Sustainable Future.

Valera-Medina, A., Xiao, H., Owen-Jones, M., David, W., Bowen, P., 2018. Ammonia for power. Progress in Energy and Combustion Science 69, 63 – 102. URL: http://www.sciencedirect.com/science/article/pii/S0360128517302320, doi:https://doi.org/10.1016/j.pecs.2018.07.001.

Wang, G., Mitsos, A., Marquardt, W., 2017. Conceptual design of ammonia-based energy storage system: System design and time-invariant performance. AIChE Journal 63, 1620–1637. URL: https://aiche.onlinelibrary.wiley.com/doi/abs/10.1002/aic.15660, doi:10.1002/aic.15660, arXiv:https://aiche.onlinelibrary.wiley.com/doi/pdf/10.1002/aic.15660.

Wang, L., Zhang, Y., Pérez-Fortes, M., Aubin, P., Lin, T.E., Yang, Y., Maréchal, F., Van herle, J., 2020. Reversible solid-oxide cell stack based power-to-x-to-power systems: Comparison of thermodynamic performance. Applied Energy 275, 115330. URL: http://www.sciencedirect.com/science/article/pii/S0306261920308424, doi:https://doi.org/10.1016/j.apenergy.2020.115330.

Zhang, C., Greenblatt, J.B., Wei, M., Eichman, J., Saxena, S., Muratori, M., Guerra, O.J., 2020. Flexible grid-based electrolysis hydrogen production for fuel cell vehicles reduces costs and greenhouse gas emissions. Applied Energy 278, 115651. URL: http://www.sciencedirect.com/science/article/pii/S0306261920311491, doi:https://doi.org/10.1016/j.apenergy.2020.115651.

Zhang, Y., Wang, L., Wang, N., Duan, L., Zong, Y., You, S., Maréchal, F., Van herle, J., Yang, Y., 2019. Balancing wind-power fluctuation via onsite storage under uncertainty: Power-to-hydrogen-to-power versus lithium battery. Renewable and Sustainable Energy Reviews 116, 109465. URL: http://www.sciencedirect.com/science/article/pii/S1364032119306732, doi:https://doi.org/10.1016/j.rser.2019.109465.

Zhao, Y., Setzler, B.P., Wang, J., Nash, J., Wang, T., Xu, B., Yan, Y., 2019. An efficient direct ammonia fuel cell for affordable carbon-neutral transportation. Joule 3, 2472–2484. URL: https://www.sciencedirect.com/science/article/pii/S2542435119303216, doi:https://doi.org/10.1016/j.joule.2019.07.005.

Zhu, J., Meng, X., Zhao, J., Jin, Y., Yang, N., Zhang, S., Sunarso, J., Liu, S., 2017. Facile hydrogen/nitrogen separation through graphene oxide membranes supported on ysz ceramic hollow fibers. Journal of Membrane Science 535, 143 – 150. URL: http://www.sciencedirect.com/science/article/pii/S037673881730234X, doi:https://doi.org/10.1016/j.memsci.2017.04.032.